Frost, Ray and Muscemeci, Anthony and Martens, Wayde and Adebajo, Moses and Bouzaid, Jocelyn (2005) Raman spectroscopy of hydrotalcites with sulphate, molybdate and chromate in the interlayer. *Journal of Raman Spectroscopy* 36(10):pp. 925-931.

Raman spectroscopy of hydrotalcites with sulphate, molybdate and chromate in the interlayer

Ray L. Frost•, Anthony W. Musumeci, Wayde N. Martens, Moses O. Adebajo and Jocelyn Bouzaid

Inorganic Materials Research Program, School of Physical and Chemical Sciences, Queensland University of Technology, GPO Box 2434, Brisbane Queensland 4001, Australia.

Abstract

Raman microscopy has been used to characterize the interlayer anions in synthesized hydrotalcites of formula $Mg_6Al_2(OH)_{16}(XO_4).4H_2O$ where X is S or Mo or Cr. The Raman spectroscopy shows that both the chromate and molybdate anions are not polymerised in the hydrotalcite interlayer. This lack of polymerisation is attributed to the effect of pH during synthesis. A model of bonding is proposed for the interlayer anions based upon the observation of two symmetric stretching modes and symmetry lowering of the chromate, molybdate and sulphate anions. Two types of anions are present hydrated and hydroxyl surface bonded.

Key Words: hydrotalcite, brucite, Raman microscopy, carrboydite, hydrohonessite, takovite, mountkeithite.

INTRODUCTION

Hydrotalcites both natural and synthetic have been known for an extended period of time [1-3]. Early reports of natural hydrotalcites date back to 1944 [4]. Hydrotalcites, or layered double hydroxides (LDH) are fundamentally known as anionic clays, and are less well-known and more diffuse in nature than cationic clays such as smectites [5]. In the laboratory using a number of techniques LDH's may be synthesized. Interest in the study of hydrotalcites results from their potential use as catalysts [6-10]. The reason rests with the ability to make mixed metal oxides at the atomic level, rather than at a particle level. Such mixed metal oxides are formed through the thermal decomposition of the hydrotalcite. [11,12] Hydrotalcites may also be used as components in new nano-materials such as nano-composites. [13] There are many other uses of hydrotalcites such as in the removal of environmental hazards in acid mine drainage [14,15]. Hydrotalcite formation offers a mechanism for the disposal

• Author to whom correspondence should be addressed (r.frost@qut.edu.au)

of radioactive wastes [16] and may also serve as a means of heavy metal removal from contaminated waters [17].

The structure of hydrotalcite can be derived from a brucite structure ($Mg(OH)_2$) in which e.g. Al^{3+} or Fe^{3+} (pyroaurite-sjögrenite) substitutes a part of the Mg^{2+} [2,18-20]. This substitution creates a positive layer charge on the hydroxide layers, which is compensated by interlayer anions or anionic complexes. For synthetic LDH's any anion may be used. Anions such as chloride, nitrate, chromate, molybdate are suitable. In hydrotalcites a broad range of compositions are possible of the type $[M^{2+}_{1-x}M^{3+}_{x}(OH)_2]_{x/n}.yH_2O$, where M^{2+} and M^{3+} are the di- and trivalent cations in the octahedral positions within the hydroxide layers with x normally between 0.17 and 0.33. A^{n-} is an exchangeable interlayer anion [21]. There exists in nature a significant number of hydrotalcites which are formed as deposits from ground water containing Ni^{2+} and Fe^{3+} [22]. These are based upon the dissolution of Ni-Fe sulphides during weathering. Among these naturally occurring hydrotalcites are carrboydite and hydrohonessite [23,24]. These two hydrotalcites are based upon the incorporation of sulphate into the interlayer with expansions of 10.34 to 10.8 Å. Normally the hydrotalcite structure based upon takovite (Ni,Al) and hydrotalcite (Mg,Al) has basal spacings of ~8.0 Å where the interlayer anion is carbonate. The spacing in the interlayer depends simply on the size of the interlayer anion.

The characterisation of these types of minerals by infrared spectroscopy has been well documented. [6] More recently, infrared emission spectroscopy has been used to study the thermal behaviour of hydrotalcites. One of the disadvantages of infrared spectroscopy in the study of hydrotalcites is that the water in the hydrotalcite is such an intense absorber, and may mask the absorbance of the MOH units. One of the advantages of Raman spectroscopy is that water is a very poor scatterer. Thus the hydroxyl stretching of the MOH units may be readily observed. However few reports of the Raman spectroscopy of these hydrotalcite minerals either natural or synthetic have been forthcoming. The application of Raman spectroscopy to the study of synthetic Co/Al and Ni/Al hydrotalcites has shown the reduced symmetry of the carbonate in the interlayer [25]. The effect of cation size on hydrotalcite stability has been studied using vibrational spectroscopic techniques [26]. In-situ infrared and Raman spectroscopy has been used to determine the thermal stability of as-synthesised Co/Al and Ni/Al hydrotalcites [25,26]. In this paper, we report the anion chemistry of sulphate, molybdate and chromate in the interlayer of hydrotalcite using Raman microscopy.

EXPERIMENTAL

Synthesis of hydrotalcite compounds:

A mixed solution of aluminium and magnesium nitrates ($[Al^{3+}]$ = 0.25M and $[Mg^{2+}]$ = 0.75M; 1M = 1mol/dm^3) and a mixed solution of sodium hydroxide ($[OH^-]$ = 2M) and the desired anion, at the appropriate concentration, were placed in two separate vessels and purged with nitrogen for 20 minutes (all compounds were dissolved in freshly decarbonated water). The cationic solution was added to the anions via a peristaltic pump at 40mL/min and the pH maintained above 9. The mixture was then aged at 75°C for 18 hours under a N_2 atmosphere. The resulting precipitate was then filtered thoroughly with room temperature decarbonated water to remove nitrates and left to dry in a vacuum desiccator for several days. In this way

hydrotalcites with different anions in the interlayer were synthesised. The phase composition was checked by X-ray diffraction and the chemical composition by EDXA analyses.

X-ray diffraction

X-Ray diffraction patterns were collected using a Philips X'pert wide angle X-Ray diffractometer, operating in step scan mode, with Cu K_α radiation (1.54052 Å). Patterns were collected in the range 3 to 90° 2θ with a step size of 0.02° and a rate of 30s per step. Samples were prepared as a finely pressed powder into aluminium sample holders. The Profile Fitting option of the software uses a model that employs twelve intrinsic parameters to describe the profile, the instrumental aberration and wavelength dependent contributions to the profile.

Infrared spectroscopy

Infrared spectra were obtained using a Nicolet Nexus 870 FTIR spectrometer with a smart endurance single bounce diamond ATR cell. Spectra over the 4000–525 cm^{-1} range were obtained by the co-addition of 64 scans with a resolution of 4 cm^{-1} and a mirror velocity of 0.6329 cm/s. Spectra were co-added to improve the signal to noise ratio.

Raman microprobe spectroscopy

The crystals of hydrotalcite minerals were placed and orientated on a polished metal surface on the stage of an Olympus BHSM microscope, which is equipped with 10x and 50x objectives. The microscope is part of a Renishaw 1000 Raman microscope system, which also includes a monochromator, a filter system and a Charge Coupled Device (CCD). Raman spectra were excited by a Spectra-Physics model 127 He-Ne laser (633 nm) at a resolution of 2 cm^{-1} in the range between 100 and 4000 cm^{-1}. Repeated acquisition, using the highest magnification, was accumulated to improve the signal to noise ratio in the spectra. Spectra were calibrated using the 520.5 cm^{-1} line of a silicon wafer. Powers of less than 1 mW at the sample were used to avoid laser induced degradation of the sample [27-29]. Slight defocusing of the laser beam also assists in the preservation of the sample.

Spectroscopic manipulation such as baseline adjustment, smoothing and normalisation were performed using the Spectracalc software package GRAMS (Galactic Industries Corporation, NH, USA). Band component analysis was undertaken using the Jandel 'Peakfit' software package, which enabled the type of fitting function to be selected and allows specific parameters to be fixed or varied accordingly. Band fitting was done using a Gauss-Lorentz cross-product function with the minimum number of component bands used for the fitting process. The Gauss-Lorentz ratio was maintained at values greater than 0.7 and fitting was undertaken until reproducible results were obtained with squared correlations of r^2 greater than 0.995.

RESULTS AND DISCUSSION

X-ray diffraction

The X-ray diffraction patterns of the hydrotalcite of formula $(Mg_6Al_2(OH)_{16}(XO_4).4H_2O)$ where X is S, Cr or Mo is shown in Figure 1. The d(003) spacing for the sulphate, chromate and molybdate interlayered hydrotalcites are 7.99, 7.98 and 7.97 Å respectively. Such values are close to the d-spacing values reported for the natural hydrotalcite with sulphate in the interlayer.
The XRD of the products of the thermal decomposition of the chromate hydrotalcite shows that MgO (JCPD file 45-0946), Cr_2O_3 (01-1294) and spinel (75-1798) are formed. The products of the thermal decomposition of the molybdate-hydrotalcite were MgO, $MgMoO_4$ (21-0961) and $MgAl_2O_4$. The products of the sulphate-hydrotalcite were a mixture of the oxides of Mg and Al. These types of products are in agreement with published data [30].

Sulphate vibrations

The free sulphate anion SO_4^{2-} has a site symmetry of T_d corresponding to a space group of O_h^7 with the $\nu_3(F)$ and $\nu_4(F)$ modes both Raman and infrared active, while the $\nu_1(A_1)$ and $\nu_2(E)$ modes are only Raman active with ν_1 around 981, ν_2 around 451, ν_3 around 1104 and ν_4 around 613 cm^{-1}. Good examples of hydrotalcites with sulphate in the interlayer are honessite, hydrohonessite and carrboydite. The Raman spectrum of the SO_4^{2-}, MoO_4^{2-} and CrO_4^{2-} in the 500 to 1200 cm^{-1} region are shown in Figure 2. The results of the Raman spectroscopic analyses are reported in Table 1.

The Raman spectrum of the SO_4^{2-} stretching region shows an intense band at 982 cm^{-1} which may be curve resolved into two components at 983.7 and 979.6 cm^{-1}. The bands are narrow with bandwidths of 12.2 and 7.7 cm^{-1}. These bands are assigned to the SO_4^{2-} symmetric stretching vibrations. The first band may be assigned to the hydrated SO_4^{2-} ion and the second band to a SO_4^{2-} unit which is hydrogen bonded to the hydrotalcite hydroxyl surface. In contrast the natural mineral carrboydite is characterised by an intense band centred at 981 cm^{-1} with bandwidth of 28.7 cm^{-1}. In the case of hydrohonessite and reevesite, the Raman spectrum show sharp bands at 1008 cm^{-1} with bandwidths of 5.5 cm^{-1}. The Raman spectrum of the SO_4^{2-} unit in the synthetic hydrotalcite shows a band at 1044.4 cm^{-1}. The intensity of the band is very low for the synthetic sulphate interlayered hydrotalcite. This band is attributed to the antisymmetric stretching vibrations. In the case of the natural mineral carrboydite a very broad band for carrboydite is observed at around 1125 cm^{-1}.The infrared spectrum of carrboydite shows three bands at 1088, 1021 and 978 cm^{-1}. The first two bands are due to the intense SO_4 antisymmetric stretching vibrations and the last band is the weak infrared SO_4 symmetric stretching vibration. Hydrohonessite Raman spectrum shows two bands at 1135 and 1115 cm^{-1} with bandwidths of 8.2 and 26.1 cm^{-1}. The reevesite Raman spectrum displays two bands at 1135 and 1118 cm^{-1} with bandwidths of 10.4 and 16.7 cm^{-1}. The Raman spectrum of mountkeithite

displays two bands at 1129 and 1109 cm^{-1}, assigned to the SO_4^{2-} antisymmetric stretching vibrations.

The Raman spectrum of the SO_4^{2-} low wavenumber region shows two bands at 715 and 615 cm^{-1} (Figures 2 and 3). These bands are quite broad with bandwidths of 22.2, and 43.5 cm^{-1}. These bands are attributed to the SO_4^{2-} ν_4 bending modes. Two additional bands are observed at 465 and 444 cm^{-1} with bandwidths of 34.1 and 18.7 cm^{-1} and are attributed to the ν_2 bending modes. In comparison, for carrboydite, the ν_4 bands are observed at 631, 613, 563 and 552 cm^{-1} with bandwidths of 28.9, 30.2, 46.5 and 15.5 cm^{-1}. The ν_2 bands for carrboydite are observed at 499, 457 and 403 cm^{-1}. The Raman spectrum of hydrohonessite displayed bands at 671, 619 and 579 cm^{-1}. The Raman bands for reevesite are observed at 670, 619 and 586 cm^{-1} for the ν_4 vibrations with bandwidths of 6.3, 12.7 and 53.2 cm^{-1}. The ν_2 modes for reevesite are observed at 493 and 414 cm^{-1} with bandwidths of 10.3 and 8.1 cm^{-1}. The bands at 383 and the set of bands at around 200 cm^{-1} are attributed to metal-oxygen vibrations.

The Raman spectrum of the OH stretching region is shown in Figure 4. Five bands are observed at 3686, 3642, 3610 cm^{-1} ascribed to the cation-OH stretching vibrations and at 3479 and 3270 cm^{-1} assigned to water stretching vibrations. A model is proposed based upon a tripod of M_3OH units in the hydrotalcite structure. In a simplified model, Raman spectra of the hydroxyl-stretching region enable bands to be assigned to the Mg_3OH. Al_3OH and $MgAl_2OH$ units. In brucite type solids, there are tripod units M_3OH with several metals such as M, M', M". In hydrotalcites such as those based upon Mg of formula $Mg_6Al_2(OH)_{16}(SO_4).4H_2O$, a number of statistical permutations of the M_3OH units are involved. These are Mg_3OH, Al_3OH and combinations such as Mg_2AlOH, Al_2MgOH. These types of units will be distributed according to a probability distribution according to the composition. In this model, a number of assumptions are made, namely that the molecular assembly is random and that no islands or lakes of cations are formed. In a somewhat oversimplified model, for the $Mg_6Al_2(OH)_{16}(SO_4).4H_2O$ hydrotalcite, the most intense bands would be due to the Mg_3OH and Al_3OH bands. The ratio of intensities of the bands at 3686, 3642 and 3610 cm^{-1} is 9.2/3.3/4.0. i.e. approximately 3/1/1. Thus the assignment of these three bands is to the Mg_3OH, Mg_2AlOH and Al_3OH stretching vibrations.

Bish and Livingstone observed for honessite the sulphate ν_1, ν_2, ν_3 and ν_4 modes at 980, 500, 1140 and 650 cm^{-1}, respectively. [23] The ν_3 mode is clearly split but no separate band positions were given. The infrared spectrum of synthetic hydrohonessite was very similar to that of the naturally occurring honessite. [23] Although the split of the ν_3 mode is only visible as a weak shoulder on the low wavenumber side of the comparatively broad band in contrast to the (hydro)honessite, where the weaker of the two bands is observed as a separate band or shoulder at the higher wavenumber side. The fact that these authors found all four modes to be infrared active indicates that the symmetry of the sulphate anion has been lowered from T_d for the free anion to C_3 or C_{3v}, which would result in activation of the two infrared inactive modes plus splitting of the ν_3 mode. Dutta and Puri observed bands associated with the sulphate anion in Li/Al-hydrotalcite in the Raman spectrum around 457, 467, 620 (all three weak), 986 and 1116 cm^{-1} (broad). The splitting of ν_2 and the broadening of the antisymmetric stretching mode ν_3 indicate a significant

symmetry lowering. [31] Dutta and Puri suggested D_2 which is however not compatible with the infrared data where all four bands have been observed. [31] For similar reasons C_3 site symmetry as suggested by Bish is not compatible with the Raman data. Therefore, based on combined observations in both the infrared and Raman spectra the conclusion has to be that the site symmetry is most probably C_{2v} or C_s with $\nu_1(A_1)$ infrared and Raman active, $\nu_2(A_1)$ infrared and Raman active, $\nu_2(A_2)$ only Raman active, and ν_3 and $\nu_4(A_1 + B_1 + B_2)$ all infrared and Raman active.

Molybdate vibrations

In aqueous systems of the MoO_4^{2-} ion, the ion has a site symmetry of T_d corresponding to a space group of O_h^7 with the $\nu_3(F)$ and $\nu_4(F)$ modes both Raman and infrared active, while the $\nu_1(A_1)$ and $\nu_2(E)$ modes are only Raman active with ν_1 around 894, ν_2 around 407, ν_3 around 833 and ν_4 at 320 cm^{-1}. [32] The Raman spectra of some molybdate containing compounds have been published [33,34]. The Raman spectrum of the molybdate anion in the hydrotalcite shows two bands at 895 and 904 cm^{-1} assigned to the MoO_4^{2-} symmetric stretching vibrations. The situation here is similar to that for the sulphate anion in the hydrotalcite interlayer. Two bands are observed indicating two different species of MoO_4^{2-} anions, one which is hydrated and a second which is bonded to the brucite-like hydroxyl surface. An additional broad band is observed at 817 cm^{-1}. This band is the ν_3 antisymmetric stretching mode. The band is very broad with a band width of 83.4 cm^{-1}. It may be decomposed into multiple bands.

The band at 472 cm^{-1} is assigned to the ν_2 bending mode. The value for the ν_2 vibration in aqueous systems is 407 cm^{-1}; thus there is significant differences between the aqueous system and the MoO_4^{2-} in the hydrotalcite interlayer. An intense band is observed at 322 cm^{-1} with a second band at 354 cm^{-1}. These two bands are assigned to the ν_4 bending modes. In aqueous systems the band is found at 320 cm^{-1}. The additional band at 354 cm^{-1} may be assigned to a second MoO_4^{2-} anion which is bonded to the brucite–like surface. The question of the effect of pH arises. MoO_4^{2-} interlayered hydrotalcites are formed under basic conditions and as a consequence the MoO_4^{2-} anion does not polymerise. Molybdate minerals are compounds containing negatively charged oxymolybdenum ions. For the most part, mineralogically speaking, the simple tetraoxomolybdate(VI) or molybdate ion, MoO_4^{2-}, is present. Under acid conditions, molybdate ions polymerize and this process can incorporate other chemical entities. Resulting heteropolymolybdates are represented in the mineral kingdom, but are rare. Indeed, only a few minerals containing essential molybdate are known. Overwhelmingly, molybdate minerals

contain the simple molybdate ion. In the case of hydrotalcites the minerals are synthesised under basic conditions and hence only the simple MoO_4^{2-} anion is found.

The Raman spectrum of the OH stretching region displays three bands at 3703, 3681 and 3629 cm^{-1}. These bands are attributed to the MOH stretching vibrations. Two additional bands are observed at 3464 and 3235 cm^{-1} which are ascribed to water stretching vibrations. The values for the MoO_4^{2-} interlayered hydrotalcite are at higher wavenumbers than for the sulphate interlayered hydrotalcite. It is suggested that the bonding of the MoO_4^{2-} anion to the hydroxyl surface is weaker than for the sulphate interlayered hydrotalcite.

Chromate vibrations

The Raman spectra of chromate anion in solution gives the ν_1 symmetric stretching mode at 848 cm^{-1}; the ν_3 mode at 884 cm^{-1}; the ν_2 mode at 348 cm^{-1} and the ν_4 mode at 363 cm^{-1}. [32] Farmer reports the infrared spectrum of barium chromate with ν_1 at 860 cm^{-1}, ν_3 at 949, 894, 873 cm^{-1} and ν_4 at 419, 389 and 375 cm^{-1}. [35] The ν_2 band was not given. The Raman spectrum of crocoite has been reported by Wilkins. [36] For crocoite all the allowed vibrations ($1A_1 + 1E + 2T_2$) are Raman active, but only the T_2 symmetry species are IR active. The Raman spectrum of the CrO_4^{2-} interlayered hydrotalcite shows an intense band at 848 cm^{-1} which is assigned to the ν_1 symmetric stretching mode. Two bands are observed at 884 and 928 cm^{-1} and are attributed to the ν_3 antisymmetric stretching mode. The bands at 363 and 237 cm^{-1} are assigned to the ν_2 bending modes. The bands at 474 cm^{-1} is due to the ν_4 bending mode. For the CrO_4^{2-} interlayered hydrotalcite, the bands are at even higher positions. The OH stretching bands for CrO_4^{2-} interlayered hydrotalcite are observed at 3691 and 3636 cm^{-1}. The water stretching vibrations are observed at 3504 and 3343 cm^{-1} for the CrO_4^{2-} system.

CONCLUSIONS

Hydrotalcites have a unique structure in that the mineral acts as an anionic clay with a 'giant' cation whose charge is counterbalanced by multiple anions in the interlayer. In nature these anions may be carbonate, chloride or sulphate depending simply what anion is available during the formation of the hydrotalcite. When synthesising LDH's of course any anion can be used and whilst sulphate is a common interlayer anion in nature, the chromate and molybdate anions are not. It is interesting that the molybdate and chromate anions do not polymerise in the interlayer as might be expected for the molybdate and to a lesser extent chromate in the interlayer. This no doubt is due to the effect of pH during synthesis. The high pH prevents polymerisation as this occurs under acidic conditions.

The observation of more than one symmetric stretching mode gives credence to the concept of two types of bonding between the XO_4 anions. Firstly the aquated anion fills the interlayer space between the brucite like sheets and secondly there is bonding of the XO_4 anions to the brucite-like hydroxyl surface. Such a model is not

unreasonable and is the basis of the bonding of carbonate anions in the hydrotalcite interlayer. The splitting of the ν_3, ν_4 and ν_2 modes indicates symmetry lowering of the chromate, molybdate and sulphate anions. The symmetry lowering must be taken into account through the bonding of the XO_4 anions to both water and the brucite-like hydroxyl surface.

Acknowledgments

The financial and infra-structure support of the Queensland University of Technology Inorganic Materials Research Program is gratefully acknowledged. The Australian Research Council (ARC) is thanked for funding.

References

1. Allmann, R. *Acta Crystallographica, Section B: Structural Crystallography and Crystal Chemistry* 1968**; 24**: 972.
2. Ingram, L, Taylor, HFW. *Mineralogical Magazine and Journal of the Mineralogical Society (1876-1968)* 1967**; 36**: 465.
3. Taylor, HFW. *Mineralogical Magazine* 1973**; 39**: 377.
4. Caillere, S. *Compt. rend.* 1944**; 219**: 256.
5. Rives, V, Editor *Layered Double Hydroxides: Present and Future*, 2001.
6. Theo Kloprogge, J, Frost, RL. *Applied Catalysis, A: General* 1999**; 184**: 61.
7. Alejandre, A, Medina, F, Rodriguez, X, Salagre, P, Cesteros, Y, Sueiras, JE. *Appl. Catal., B* 2001**; 30**: 195.
8. Das, J, Parida, K. *React. Kinet. Catal. Lett.* 2000**; 69**: 223.
9. Patel, SH, Xanthos, M, Grenci, J, Klepak, PB. *J. Vinyl Addit. Technol.* 1995**; 1**: 201.
10. Rives, V, Labajos, FM, Trujillano, R, Romeo, E, Royo, C, Monzon, A. *Appl. Clay Sci.* 1998**; 13**: 363.
11. Rey, F, Fornes, V, Rojo, JM. *J. Chem. Soc., Faraday Trans.* 1992**; 88**: 2233.
12. Valcheva-Traykova, M, Davidova, N, Weiss, A. *J. Mater. Sci.* 1993**; 28**: 2157.
13. Oriakhi, CO, Farr, IV, Lerner, MM. *Clays Clay Miner.* 1997**; 45**: 194.
14. Lichti, G, Mulcahy, J. *Chemistry in Australia* 1998**; 65**: 10.
15. Seida, Y, Nakano, Y. *Journal of Chemical Engineering of Japan* 2001**; 34**: 906.
16. Roh, Y, Lee, SY, Elless, MP, Foss, JE. *Clays and Clay Minerals* 2000**; 48**: 266.
17. Seida, Y, Nakano, Y, Nakamura, Y. *Water Research* 2001**; 35**: 2341.
18. Brown, G, Van Oosterwyck-Gastuche, MC. *Clay Minerals* 1967**; 7**: 193.
19. Taylor, HFW. *Mineralogical Magazine and Journal of the Mineralogical Society (1876-1968)* 1969**; 37**: 338.
20. Taylor, RM. *Clay Minerals* 1982**; 17**: 369.
21. Kloprogge, JT, Wharton, D, Hickey, L, Frost, RL. *American Mineralogist* 2002**; 87**: 623.
22. Nickel, EH, Wildman, JE. *Mineralogical Magazine* 1981**; 44**: 333.
23. Bish, DL, Livingstone, A. *Mineralogical Magazine* 1981**; 44**: 339.
24. Nickel, EH, Clarke, RM. *American Mineralogist* 1976**; 61**: 366.
25. Perez-Ramirez, J, Mul, G, Moulijn, JA. *Vib. Spectrosc.* 2001**; 27**: 75.
26. Perez-Ramirez, J, Mul, G, Kapteijn, F, Moulijn, JA. *J. Mater. Chem.* 2001**; 11**: 2529.
27. Martens, W, Frost, RL, Kloprogge, JT, Williams, PA. *Journal of Raman Spectroscopy* 2003**; 34**: 145.
28. Frost, RL, Martens, W, Kloprogge, JT, Williams, PA. *Journal of Raman Spectroscopy* 2002**; 33**: 801.
29. Frost, RL, Martens, WN, Williams, PA. *Journal of Raman Spectroscopy* 2002**; 33**: 475.
30. Hernandez, MJ, Ulibarri, MA, Rendon, JL, Serna, CJ. *Thermochimica Acta* 1984**; 81**: 311.
31. Dutta, PK, Puri, M. *Journal of Physical Chemistry* 1989**; 93**: 376.
32. Farmer, VC *Mineralogical Society Monograph 4: The Infrared Spectra of Minerals*, 1974.

33. Crane, M, Frost, RL, Williams, PA, Kloprogge, JT. *Journal of Raman Spectroscopy* 2002**; 33**: 62.
34. Kloprogge, JT, Frost, RL. *Neues Jahrb. Mineral., Monatsh.* 1999: 193.
35. Farmer, VC *Mineralogical Society Monograph 4: The Infrared Spectra of Minerals*; The Mineralogical Society, London, UK., 1974.
36. Wilkins, RWT. *Mineralogical Magazine* 1971**; 38**: 249.

Table 1 Raman spectroscopic analysis of the sulphate, chromate and molybdate anions in the interlayer of hydrotalcite (peak positions shown in this table result from curve resolution)

Molybdate			Chromate			Sulphate		
Peak Position/ cm^{-1}	**FWHM cm^{-1}**	**%**	**Peak Position/ cm^{-1}**	**FWHM cm^{-1}**	**%**	**Peak Position/ cm^{-1}**	**FWHM cm^{-1}**	**%**
3703.0	27.6	1.7						
3677.5	46.0	4.3	**3686.6**	40.1	2.6	**3683.3**	44.4	9.2
3629.3	93.8	4.5	**3631.0**	98.4	7.6	**3642.4**	42.8	3.3
						3610.3	83.4	4.0
			3499.2	205.4	13.7			
						3472.5	229.8	42.2
3464.7	263.4	38.5						
			3343.1	305.4	26.6			
						3270.0	224.8	13.2
3230.7	203.3	9.4						
			3054.9	285.5	5.7			
1647.0	83.0	0.6	**1665.9**	125.2	1.1			
1402.1	72.1	1.4	**1404.3**	77.0	0.6	**1393.0**	91.9	1.8
			1372.6	76.6	0.2			
1348.5	52.1	0.3						
						1127.4	58.1	1.1
						1044.4	8.4	5.1
						983.7	12.2	6.2
						979.6	7.7	1.0
			924.7	64.5	8.1			
904.3	23.0	2.0						
895.0	16.9	7.8	**882.2**	36.4	6.2			
856.6	46.1	1.0	**846.6**	21.9	8.8			
815.5	83.4	7.1	**817.2**	104.6	6.6			
715.1	16.6	0.4	**709.7**	31.5	0.4	**711.4**	22.2	0.7
						611.5	43.5	1.2
468.6	42.4	2.1	**469.9**	27.3	0.3	**464.8**	34.1	2.2
						444.3	18.7	0.4
						381.4	27.6	0.3
351.4	86.0	2.0	**359.1**	51.3	5.6			
			337.1	14.2	0.3			
320.2	42.4	6.7						
						267.6	10.6	0.1
250.8	72.7	1.2						
			237.0	53.5	0.4	**239.1**	38.4	0.3
						221.7	9.1	0.1
198.2	27.9	0.4	**198.7**	24.0	0.6	**198.4**	29.5	0.7

List of Figures

Figure 1 X-ray diffraction of hydrotalcite with SO_4^{2-}, MoO_4^{2-} and CrO_4^{2-} in the interlayer.

Figure 2 Raman spectra in the 650 to 1200 cm^{-1} region of hydrotalcite with SO_4^{2-}, MoO_4^{2-} and CrO_4^{2-} in the interlayer.

Figure 3 Raman spectra in the 100 to 650 cm^{-1} region of hydrotalcite with SO_4^{2-}, MoO_4^{2-} and CrO_4^{2-} in the interlayer.

Figure 4 Raman spectra in the 2800 to 3800 cm^{-1} region of hydrotalcite with SO_4^{2-}, MoO_4^{2-} and CrO_4^{2-} in the interlayer.

List of Tables

Table 1 Raman spectroscopic analysis of the sulphate, chromate and molybdate anions in the interlayer of hydrotalcite

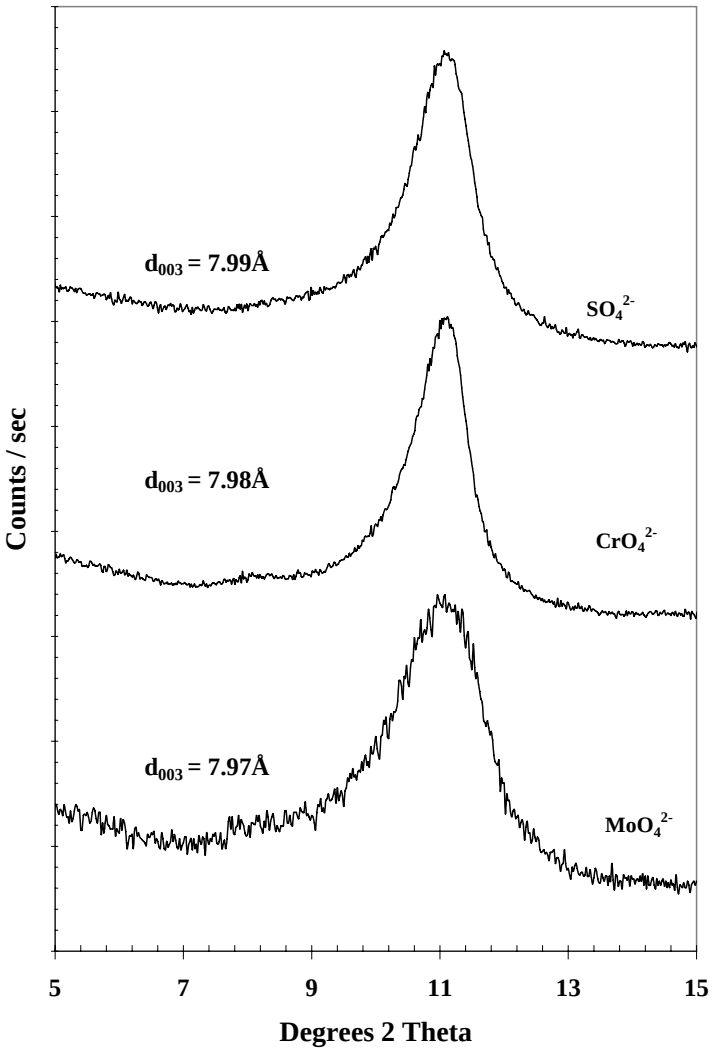

Figure 1 X-ray diffraction patterns of the d(003) spacing of hydrotalcite with different anions in the interlayer.

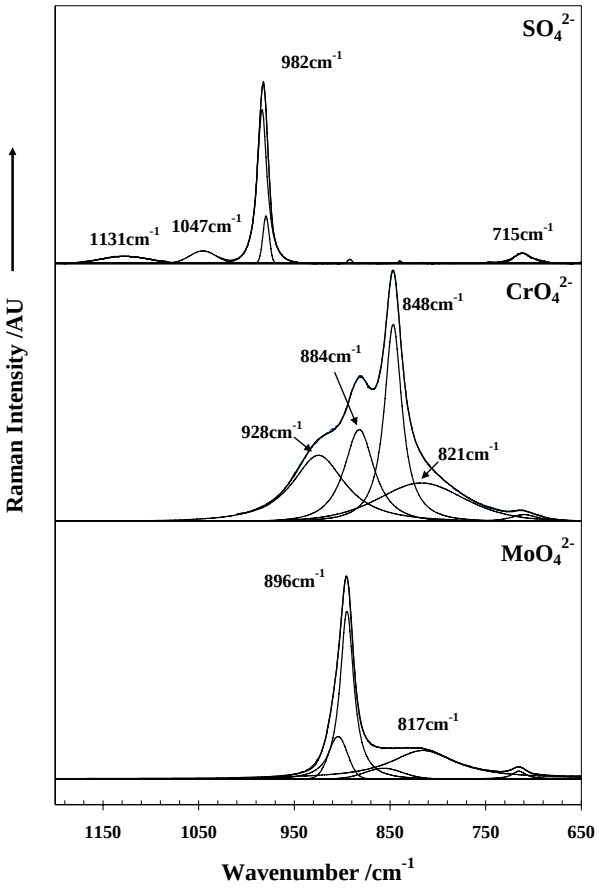
SO4 2-
982cm-1
1131cm-1
1047cm-1
715cm-1
CrO4 2-
848cm-1
884cm-1
928cm-1
821cm-1
MoO4 2-
896cm-1
817cm-1
Raman Intensity /AU
1150
1050
950
850
750
650
Wavenumber /cm-1

Figure 2

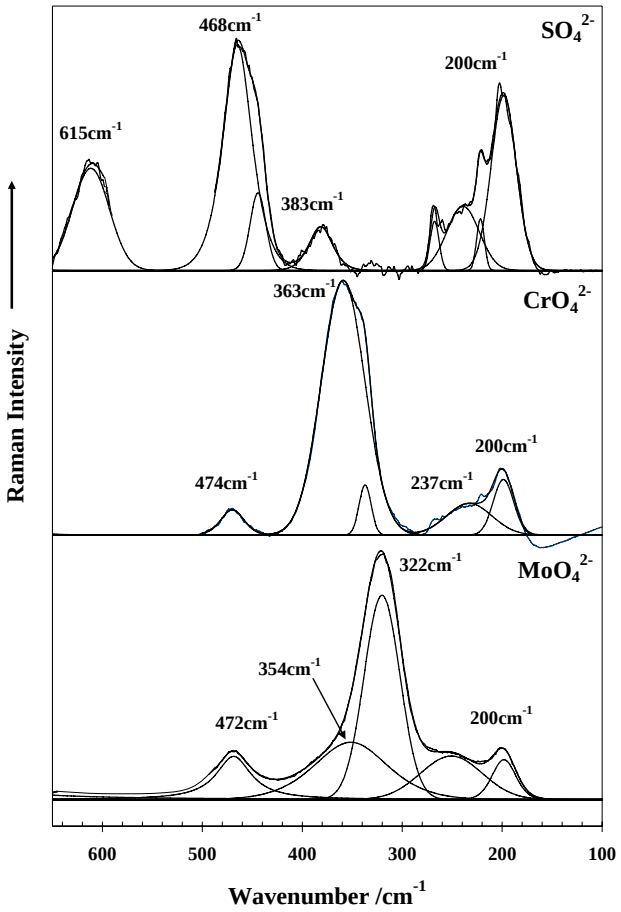
468cm-1
SO4 2-
200cm-1
615cm-1
383cm-1
363cm-1
CrO4 2-
200cm-1
474cm-1
237cm-1
322cm-1
MoO4 2-
354cm-1
472cm-1
200cm-1
Raman Intensity
600
500
400
300
200
100
Wavenumber /cm-1

Figure 3

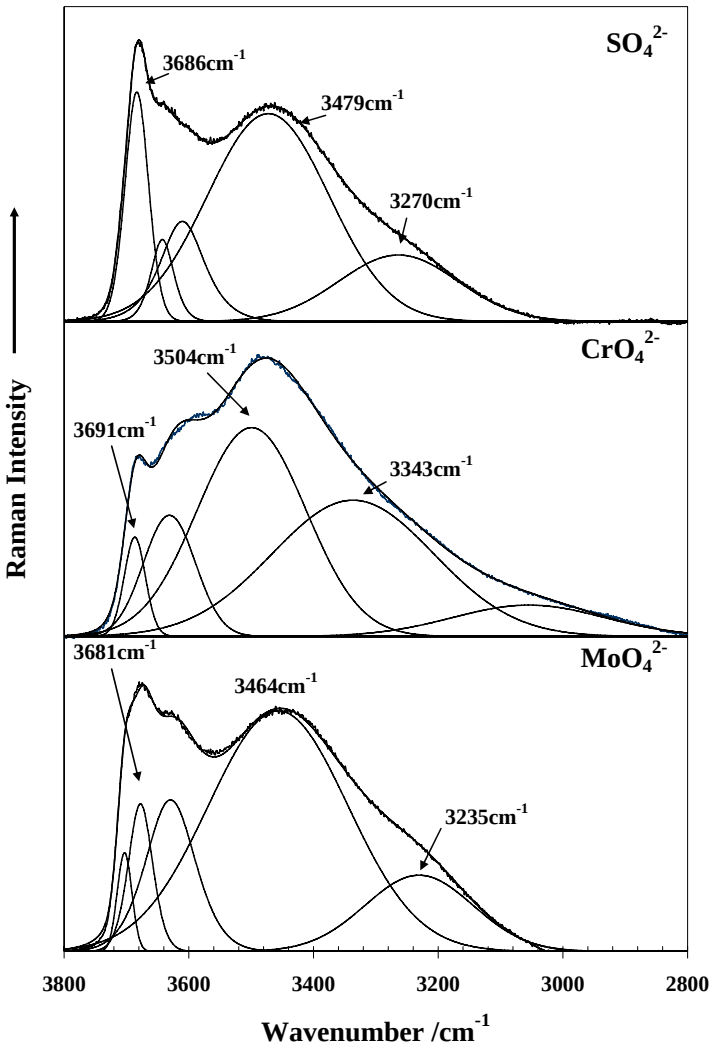
SO4 2-
3686cm-1
3479cm-1
3270cm-1
CrO4 2-
3504cm-1
3691cm-1
3343cm-1
MoO4 2-
3681cm-1
3464cm-1
3235cm-1
Raman Intensity
3800
3600
3400
3200
3000
2800
Wavenumber /cm-1

Figure 4